AD-A151 512 FURTHER DEVELOPMENTS OF THE MOMENTUM INTEGRAL METHOD FOR BOUNDARY LAYERS(U) SCIENCE APPLICATIONS INC ANNAPOLIS MD C H VON KERCZEK ET AL. 16 MAY 84 1/1

UNCLASSIFIED SAI-84/3046 N00014-81-C-0234 F/G 20/4 NL

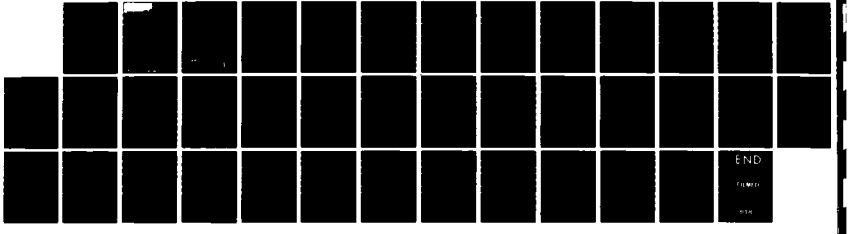

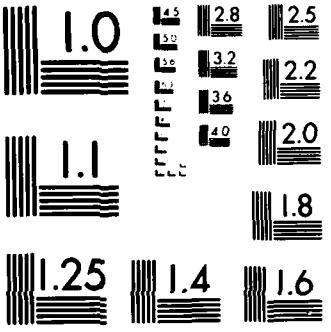

FURTHER DEVELOPMENTS OF THE MOMENTUM INTEGRAL METHOD FOR SHIP BOUNDARY LAYERS

SAI-84/3046

SCIENCE APPLICATIONS, INC.

FURTHER DEVELOPMENTS OF THE MOMENTUM INTEGRAL METHOD FOR SHIP BOUNDARY LAYERS

SAI-84/3046

SAIC
Science Applications International Corporation
134 Holiday Court, Suite 318, Annapolis, Maryland 21401, (301) 266-0991

FURTHER DEVELOPMENTS OF THE MOMENTUM INTEGRAL METHOD FOR SHIP BOUNDARY LAYERS

SAI-84/3046

Contract #N00014-81-C-0234

16 May 1984

Submitted to

David W. Taylor Naval Ship
Research & Development Center
Code 1505
Bethesda, MD

Submitted by

C. von Kerczek, G. Christoph
and F. Stern

SCIENCE APPLICATIONS, INC.

134 Holiday Court, Suite 318
Annapolis, Maryland 21401
(301) 266-0991; D.C. 261-8026

UNCLASSIFIED

SECURITY CLASSIFICATION OF THIS PAGE (When Data Entered)

REPORT DOCUMENTATION PAGE		READ INSTRUCTIONS BEFORE COMPLETING FORM
1. REPORT NUMBER	2. GOVT ACCESSION NO. AD-A155 152	3. RECIPIENT'S CATALOG NUMBER
4. TITLE (and Subtitle) FURTHER DEVELOPMENTS OF THE MOMENTUM INTEGRAL METHOD FOR SHIP BOUNDARY LAYERS		5. TYPE OF REPORT & PERIOD COVERED Final 2/4/81 - 5/1/84
		6. PERFORMING ORG. REPORT NUMBER SAI-84/3046
7. AUTHOR(s) C.H. von Kerczek, G. Christoph & F. Stern		8. CONTRACT OR GRANT NUMBER(s) N00014-81-C-0234
9. PERFORMING ORGANIZATION NAME AND ADDRESS Science Applications, Inc. 134 Holiday Court, Suite 318 Annapolis, MD 21401		10. PROGRAM ELEMENT, PROJECT, TASK AREA & WORK UNIT NUMBERS
11. CONTROLLING OFFICE NAME AND ADDRESS David W. Taylor Naval Ship Research and Development Center, Code 1505 Bethesda, MD 20084		12. REPORT DATE 16 May 1984
		13. NUMBER OF PAGES 32
14. MONITORING AGENCY NAME & ADDRESS (if different from Controlling Office) Office of Naval Research 800 N. Quincy Street Arlington, VA 22217		15. SECURITY CLASS. (of this report) Unclassified
		15a. DECLASSIFICATION/DOWNGRADING SCHEDULE N/A

16. DISTRIBUTION STATEMENT (of this Report)

Approved for public release, distribution unlimited.

17. DISTRIBUTION STATEMENT (of the abstract entered in Block 20, if different from Report)

18. SUPPLEMENTARY NOTES

This research was sponsored by the Naval Sea Systems Command General Hydrodynamics Research Program, administered by the David W. Taylor Naval Ship Research and Development Center (Code 1505), Bethesda, MD 20084.

19. KEY WORDS (Continue on reverse side if necessary and identify by block number)

GHR Program, Turbulence, Boundary Layers, Ships, Viscous Drag, 3-Dimensional.

20. ABSTRACT (Continue on reverse side if necessary and identify by block number)

This report describes three phases of work towards improving and extending the three-dimensional ship boundary layer calculation method of von Kerczek (1982), developed under prior GHR support. The three items discussed in this report are the following: (1) the method has been extended to deal with roughness of the ship hull; (2) a viscous inviscid interaction scheme has been developed but not yet computationally implemented; and (3) the computer implementation of the basic von Kerczek momentum integral method has been improved in several details. These are described in this report.

DD FORM 1 JAN 73 1473 EDITION OF 1 NOV 65 IS OBSOLETE

S/N 0102-LF-014-6601

UNCLASSIFIED

SECURITY CLASSIFICATION OF THIS PAGE (When Data Entered)

TABLE OF CONTENTS

ABSTRACT

This report describes three phases of work towards improving and extending the three-dimensional ship boundary layer calculation method of von Kerczek (1982) developed under prior GHR support. The three items discussed in this report are the following: (1) the method has been extended to deal with roughness of the ship hull; (2) a viscous inviscid interaction scheme has been developed but not yet computationally implemented; and (3) the computer implementation of the basic von Kerczek momentum integral method has been improved in several details. These are described in this report.

1.0 INTRODUCTION

Under prior GHR support von Kerczek (1982) (henceforth referred to as K) developed a momentum integral ship boundary layer calculation method which seems to be a promising, relatively simple and useful way of estimating the viscous flow and some of its consequences. This method is capable of dealing with reversed cross-flow boundary layer velocity profiles and thus can be made more acucrate than prior momentum integral methods for ships (see von Kerczek and Langan, 1979).

The method of K has already been put to use to calculate the total drag of a destroyer hull (von Kerczek, et al., 1983) and as an aid in determining appendage drag (Stern and von Kerczek, 1983). These applications are still tentative and require further verification and refinement. However, the results are encouraging and also have pointed the way towards some of the more important weaknesses of the method of K.

Under further GHR support, for which this report is presented, three items have been considered to improve the K method. These are the following:

(1) The method of K has been extended to deal with roughness of the ship hull.

(2) A method for viscous-inviscid interaction has been developed, but not yet computationally implemented.

(3) The computer implementation of the basic method of K has been improved in several details making it more reliable and accurate.

This report details each of these efforts.

2.0 A GENERAL PROCEDURE FOR INCLUDING ROUGHNESS EFFECTS IN THE INTEGRAL BOUNDARY LAYER EQUATIONS

2.1 Introduction

Most roughness analyses are based on Nikuradse's sand-grain experiments and fitting of the law-of-the-wall velocity profiles to experimental data. Several correlations have been proposed to relate real roughness heights, spacings and geometries to an equivalent sand-grain height so that Nikuradse's data can be used. Examples of such correlations can be found in Betterman (1966), Simpson (1973) and Dirling (1973). These correlations are not very accurate for closely spaced roughness elements such as those found on a ship's surface. The correlations in these references are biased toward data for roughness elements with large spacings.

More meaningful methods that account for actual roughness effects are those employed by Christoph and Pletcher (1983), Finson and Clarke (1980) and Lin and Bywater (1982). These techniques calculate the form-drag contributions of individual elements. Roughness elements are assumed to occupy no physical space. The governing boundary layer equations are cast in a form to account for the blockage effects of the roughness elements. Terms that act in the streamwise direction are multiplied by the factor $[1 - D(y)/\ell]$, where $D(y)$ is the element width at height y and ℓ is the average center-to-center spacing. Terms that act in the direction normal to the streamwise direction are multiplied by $[1 - \pi D^2(y)/(4\ell^2)]$. The effect of roughness in the momentum equations is described by a sink term and represents form drag.

To date, the form drag approach has been taken only with a finite-difference solution of the boundary layer equations. In order to apply this method directly to a 3-dimensional integral technique such as that of K, a skin friction correlation that explicitly accounts for roughness height, spacing and geometry has to be specified. This is not yet possible; instead, the following approach is taken here.

Based on results of numerous computer runs with a variety of roughness shapes and spacings, Finson (1982) suggested a correlation relating equivalent sand-grain height to roughness height, spacing and geometry. This correlation was shown by Finson to be accurate for closely packed elements. Using calculated equivalent sand-grain heights, a method was developed in this study to calculate skin friction, boundary layer thickness and velocity profiles based on classical sand-grain roughness relations. The details are described below.

2.2 Solution Procedure for 2-D Boundary Layers

It is desirable to include roughness in the full 3-D boundary layer equations using Head's entrainment technique as implemented by K. To begin the development, the roughness methodology is most easily discussed in the framework of a 2-D flow. Extension to 3-D and its implementation are discussed later. The 2-D momentum integral equation is

$$\frac{d\theta}{ds} = \frac{c_f}{2} - \theta\left(\frac{2+H}{U}\frac{dU}{ds}\right) \tag{2-1}$$

and the boundary layer entrainment equation is

$$\frac{dq}{ds} = F(G) - \frac{q}{U}\frac{dU}{ds} \tag{2-2}$$

where

$$q = G\theta \ , \ H = \delta/\theta. \tag{2-3}$$

The skin friction coefficient c_f, Head's shape factor G, and the rate of entrainment function F(G) are modelled in the same way as in K. In the present study it is assumed that roughness effects are accounted for simply by including roughness in the skin friction model. The momentum thickness θ and the shape factor H are affected by roughness through integration of equations (2-1) and (2-2). The process of entrainment is mainly controlled by the velocity defect in the outer part of the boundary layer and therefore the entrainment, as used in K, should not be affected by roughness. The

magnitude of the entrainment variables (G and F) will change, however, due to their dependence on H.

Roughness effects are modelled in c_f through the classical velocity shift, that is,

$$u_r^+ = u_s^+ - \Delta B \tag{2-4}$$

where

$$u_s^+ = \frac{1}{K} \ell n\ y^+ + \text{CONSTANT},\ K = 0.41$$

$$\Delta B = \frac{1}{K} \ell n\ k_{es}^+ - 3 \tag{2-5}$$

and

$$y^+ = yu^*/\nu,\ k_{es}^+ = k_{es}\ u^*/\nu$$

$$u^+ = u/u^*,\ u^* = (\tau_w/\rho)^{1/2}. \tag{2-6}$$

The subscripts s and r refer to smooth and rough conditions, respectively. Since

$$u_{edge}^+ = (2/c_f)^{1/2}, \tag{2-7}$$

the rough wall skin friction coefficient c_{f_r} is related to the smooth wall skin friction coefficient c_{f_s} by

$$(2/c_{f_r})^{1/2} = (2/c_{f_s})^{1/2} - \Delta B. \tag{2-8}$$

If c_{f_s} and k_{es} are known, then c_{f_r} is easily solved from equation (2-8). This is done by rewriting equation (2-8) as

$$(2/c_{f_r})^{1/2} - \frac{1}{K} \ell n\ (2/c_{f_r})^{1/2} = (2/c_{f_s})^{1/2} - \frac{1}{K} \ell n\ Re_{k_{es}} + 3$$

$$(Re_{k_{es}} = U_e\ k_{es}/\nu) \tag{2-9}$$

and using an iteration scheme, e.g., Newton-Raphson, to solve for c_{fr}. The method used for determining k_{es} is discussed next.

In the form drag analysis outlined in the introduction, the wall shear is given by

$$c_{fr} = c_{fs} + \int_0^k \frac{u^2}{u_e^2} c_D \, f(y) \, \frac{D(y)}{\ell^2} \, dy \tag{2-10}$$

where

$$f(y) = \frac{1 - D(y)/\ell}{1 - \pi D^2(y)/(4\ell^2)} \tag{2-11}$$

and c_D is a form drag coefficient. Taking $u = U_R$ = constant, c_D = constant, and evaluating $f(y)$ at $y = k/2$, equation (2-10) becomes

$$c_{fr} = c_{fs} + \frac{U_R^2}{U_e} c_D \, f(k/2)/\lambda_k. \tag{2-12}$$

The parameter

$$\lambda_k^{-1} = \text{projected frontal area of the elements per unit surface area.} \tag{2-13}$$

Based on numerous calculations for $c_D = 0.6$, c_{fs} at $Re = 10$, and $k/\theta = 1$, Finson (1982) recommends the correlation

$$\frac{U_R}{U_e} = 0.247 + 0.234 \log_{10} \lambda_k \tag{2-14}$$

So for the above conditions equation (2-12) becomes

$$c_{fr}^* = c_{fs}^* (Re_\theta = 10^5) + 0.6(0.247 + 0.234 \log_{10}\lambda_k)^2 \, f(k/2)/\lambda_k. \tag{2-15}$$

A simple relation can be obtained for the equivalent sand-grain height, k_{es}, if c_{fs} is approximated by

$$(2/c_{fs})^{1/2} = \frac{1}{K} \ell n\, Re_\theta + C \text{ (flow geometry, pressure gradient).} \quad (2\text{-}16)$$

Equation (2-9) can be rewritten as

$$(2/c_{fs})^{1/2} - \frac{1}{K} \ell n(2/c_{fr}) = \frac{1}{K} \ell n(k_{es}/\theta) + C + 3. \quad (2\text{-}17)$$

A general expression for k_{es} is obtained by using Finson's correlation ($\theta = k$) and rearranging equation (2-17) to

$$\frac{k_{es}}{k} = \exp\left[K(C + 3 - (2/c_{fr}^*)^{1/2} + \frac{1}{K}\ n(2/c_{fr}^*)^{1/2}\right]. \quad (2\text{-}18)$$

For C equal to its flat plate value of 5.5, c + 3 = 8.5. This represents flat plate flow in a fully rough regime.

2.3 Extension to 3-D

The approach taken for 3-D flows is a direct extension of the 2-D roughness analysis just discussed. The streamwise skin friction coefficient, c_{f1}, that occurs in the streamwise momentum equation is replaced by the rough wall skin friction model outlined above. Rough wall values of θ_{11}, H and θ_{21} (see K for notation) are then generated by solving equations (2-6) - (2-8) of K. The cross flow skin friction coefficient, c_{f2}, is computed from

$$c_{f2} = c_{f1} \tan\beta \quad (2\text{-}19)$$

where $\tan\beta$ is calculated from equation (5) of K. It should be noted that the rough wall skin friction calculation by equation (2-9) requires knowledge of the smooth wall skin friction. Therefore, the smooth and rough wall flows need to be calculated in parallel.

In order to obtain the crossflow boundary layer thickness, θ_{21} and θ_{12}, it is necessary to know how roughness affects the streamwise and crossflow velocity profiles. Roughness effects were included in the streamwise velocity profile as follows. Equation (2-4) is written as

$$u_r/u_r^* = u_s/u_s^* - \frac{1}{K} \ell n\ (k_{es}\ u_r^*/\nu) + 3 \qquad (2\text{-}20)$$

This is rearranged as

$$u_r/U_e = u_s/U_e\ (c_{fr}/c_{fs})^{\frac{1}{2}} + (c_{fr}/2)^{\frac{1}{2}} \left[\frac{1}{K} \ell n((2/c_{fr})^{\frac{1}{2}}) \right. \qquad (2\text{-}21)$$

$$\left. - \frac{1}{K} \ell n\ (k_{es}\ u_e/\nu) + 3\right]$$

where u_s/U_e is a smooth wall boundary layer velocity profile. For the results of this study, the profile of Kool (see K) was used. The crossflow profile is then calculated by using equation (2-21) as the streamwise profile in equation (3) of K. It is also necessary to know the rough wall nominal boundary layer thickness. It is calculated from the relation

$$\delta_r = \theta_{11}\ (G + H) \qquad (2\text{-}22)$$

where θ_{11}, G and H are rough wall values.

2.4 Computational Results

The roughness approach described above was validated by comparison to the 2-D flow roughness data of Schlichting (1937) and Healzer, Moffat and Kays (1974). First, comparisons were made to Schlichting's channel flow data where various arrangements of roughness elements were used. Figure 2-1 gives skin friction coefficient data versus distance Reynolds number (as presented by Finson and Clarke (1980)) for spherical segments with element spacings of L/D(o) = 1, 2.5 and 5. The present predictions are in excellent agreement with the data except at low Reynolds numbers and correctly predict the effect of element spacing. Figure 2-2 compares the rough wall velocity profile, equation (2-21), with profile data taken by Schlichting. The comparison of the profiles is for the top of the roughness elements out towards the edge of the boundary layer. It appears that equation (2-21) overpredicts the momentum deficit close to the wall. This overprediction is due

to the presence of the roughness elements.

The incompressible flow experiments of Healzer, et al. (1974) provide data on skin friction, heat transfer and velocity profiles for rough surfaces with and without blowing. The rough surface consisted of a regular array of tightly packed (L/D(o) = 1) hemispherical elements, each 0.05 inches in diameter. Tests were run at freestream velocities of 32, 139 and 242 ft/sec. Comparison of the skin friction coefficients are shown in Figure 2-3 for freestream velocities of 32 and 242 ft/sec. Even though the values of the calculated skin friction coefficient overpredicts the experimental values, the equivalent sand-grain height calculated from equation (2-18) is in excellement agreement with the value used by Healzer, et al. These values are 0.032 inches for the predictions as compared to 0.031 inches suggested by Healzer, et al. based on Schlichting's data. Since the roughness elements in the Healzer, et al. experiments were touching each other, it was necessary to define a new y origin. The y location at D(y) = 0.99 D(o) was arbitrarily chosen as the reference level. Velocity profile predictions and data are compared in Figure 2-4. Since predicted skin friction coefficients were high, predicted velocity profiles were normalized by the experimental edge values of u+. Again, it appears that predicted velocities are too low very near the wall. Comparisons to the rough-wall predictions for momentum thickness are shown in Figure 2-5. The increase in the values of θ due to roughness and the lesser sensitivity to freestream velocity are correctly predicted.

No rough-wall skin friction data seems to exist for 3-D flows. Therefore, only hypothetical cases could be considered. Sample cases were run for a Reynolds number representative of a full-scale ship ($RL = 2 \times 10^9$) and a Reynolds number representative of a wind tunnel model ($RL = 1 \times 10^7$). The sample ship was the same elliptic cross-section body as the sample case of K. A reference smooth wall case was run at each Reynolds number along with roughnesses defined by an equivalent sand-grain height or roughness element height, base diameter and center-to-center spacing. For the

roughness calculations it is also necessary to input a characteristic length (ship length). In the present form of the computer code only spherical segment roughness elements are considered. For the results presented here $k = 0.00083$ ft., $D(0) = 0.00167$ ft., and $\ell = 0.004175$ ft. The ship lengths used were 1000 feet for the full scale model and 10 feet for the wind tunnel model. Plots of the streamwise momentum thickness and the crossflow angle β versus arc length along the girth at $X/L = 0.84$ are given in Figures 2-6 and 2-7 for $RL = 1 \times 10^7$ and in Figures 2-8 and 2-9 for $RL = 2 \times 10^9$. As expected the momentum thickness increases with roughness. However, as shown in Figures 2-6 and 2-8, this increase is significantly less near the keel. This phenomenon is noticeable as one approaches the stern. Roughness was predicted to enhance the crossflow angle β (see Figures 2-7 and 2-9). This is especially true as the waterline is approached. Intuitively, this result was not expected. It was felt that surface roughness would tend to wash out three-dimensional effects, not enhance them. Measurements, or perhaps more exact calculations, are needed to more precisely define surface roughness effects in three-dimensional flows.

These 3-D calculations only serve the purpose of indicating that this roughness theory has been implemented and debugged in the computer programs of von Kerczek (1983) corresponding to the 3-D boundary layer theory of K. It would be very valuable to do some numerical experiments with this program. One set of tests that would be valuable is a calculation of the drag increment ΔC_D obtained by calculating the skin friction drag for a smooth and a rough hull. The form drag of Granville (1974), which only depends on C_D and the potential flow, can be used to complete the determination of ΔC_D. Although no detailed 3-D roughness boundary layer measurements seem to be available, there probably is some data (possibly for full scale ships) for which ΔC_D has been determined. For example, surely trials on a new ship and then later when the ship has aged have been performed. A thorough literature search for such cases would be highly desirable.

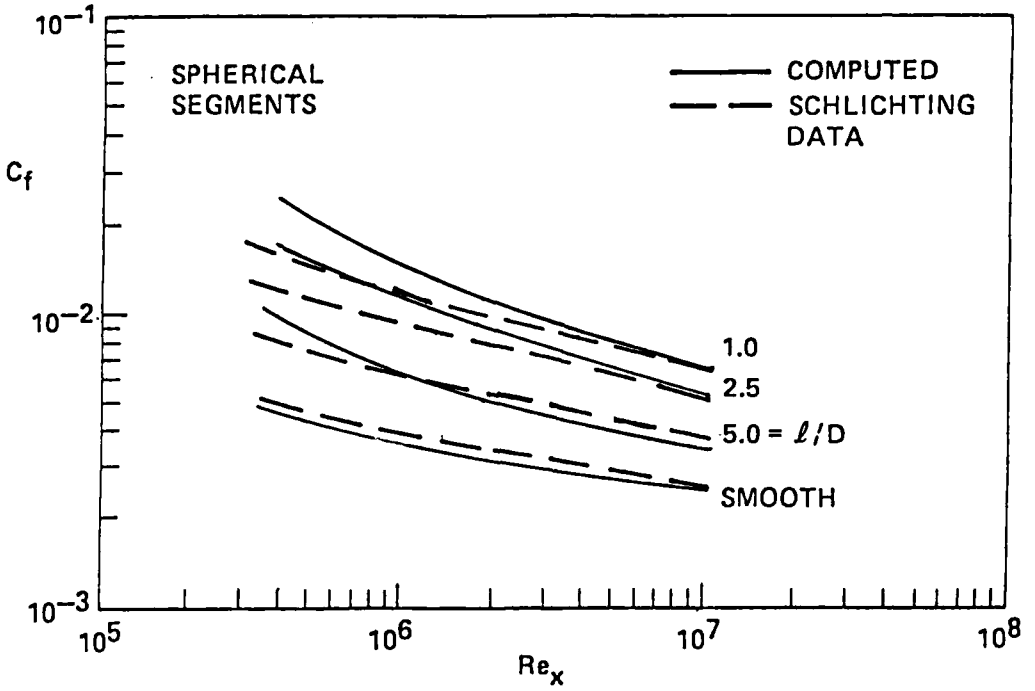

Figure 2-1. Skin-friction coefficients for Schlichting's roughness data (Schlichting, 1937).

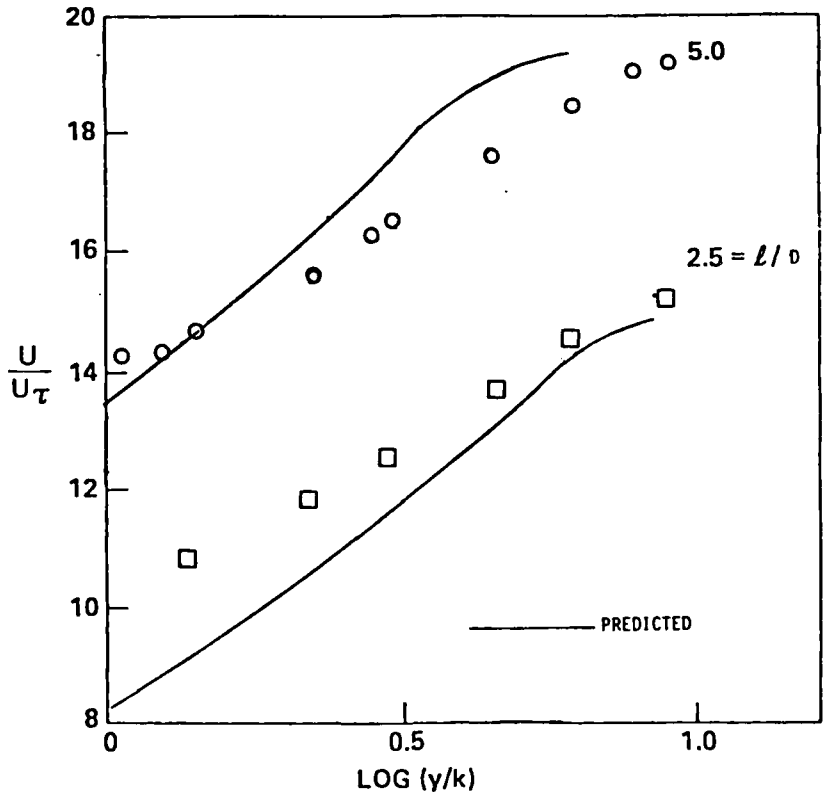

Figure 2-2. Computed mean velocity profiles compared to Schlichting's measurements for spherical segments (Schlichting, 1937)

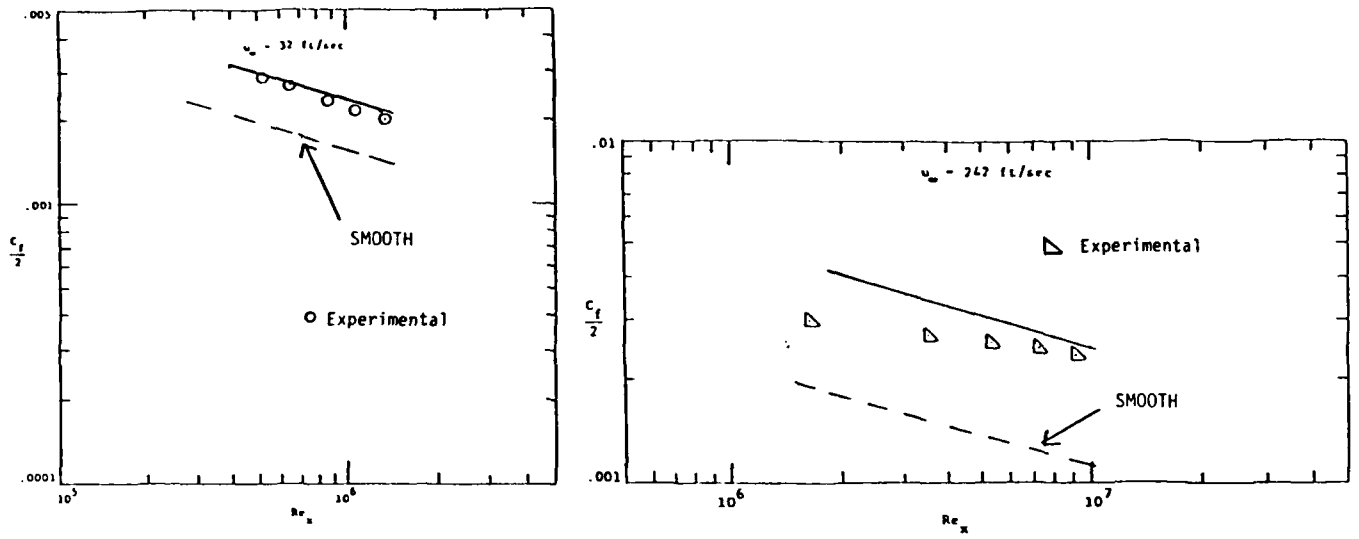

Figure 2-3. Rough surface friction versus x-Reynolds number (experimental data from Healzer, et al., 1974).

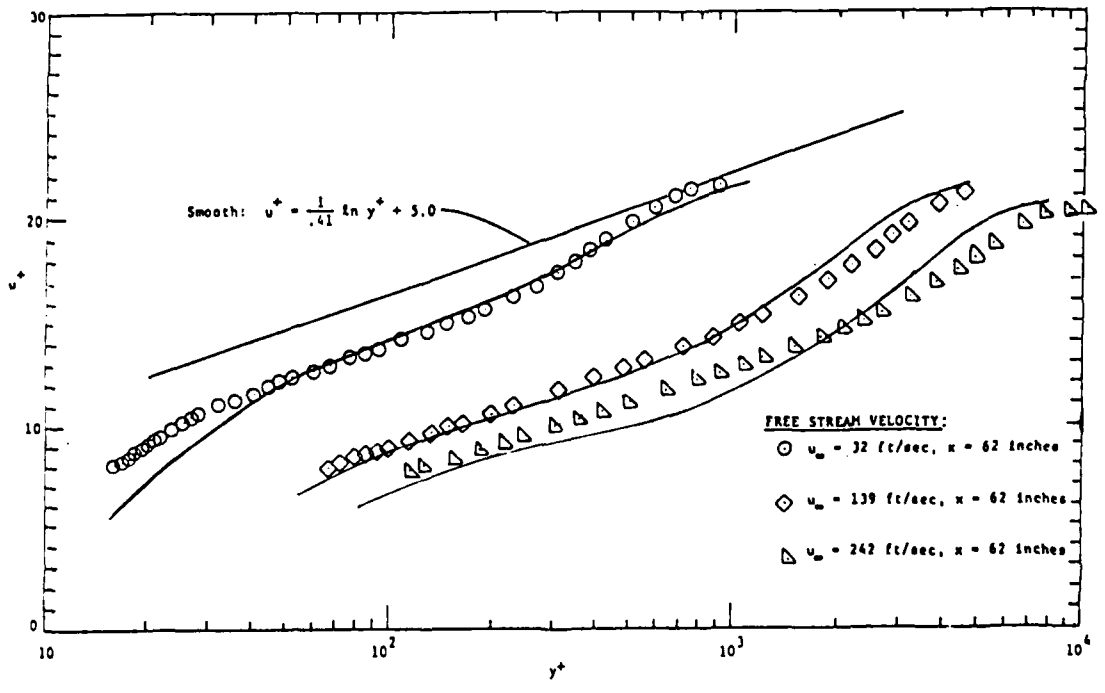

Figure 2-4. Velocity profiles at different freestream velocities (experimental data from Healzer, et al., 1974).

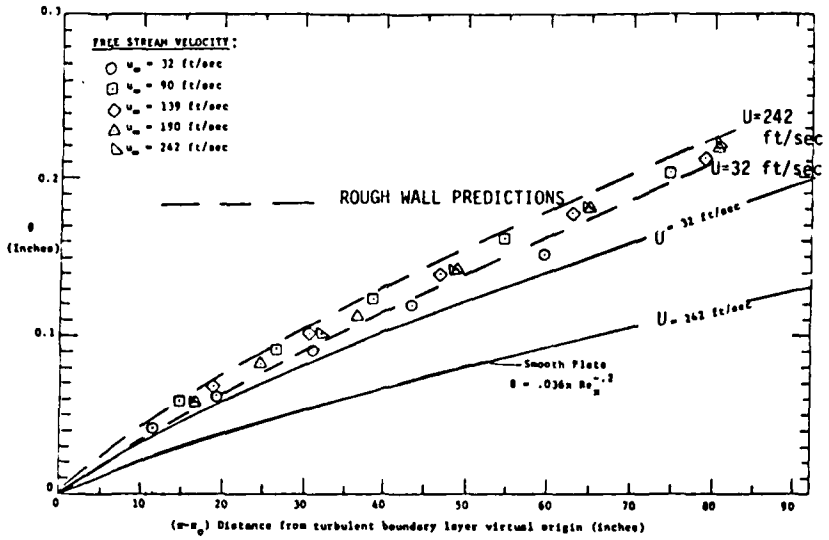

Figure 2-5. Rough surface momentum thickness versus distance (experimental data from Healzer, et al., 1974).

$R_L = 1 \times 10^7$, $k = 0.00083$ FT, $D(0) = 0.00167$ FT,
$\ell = 0.004175$ FT

$X = 0.85\,L$

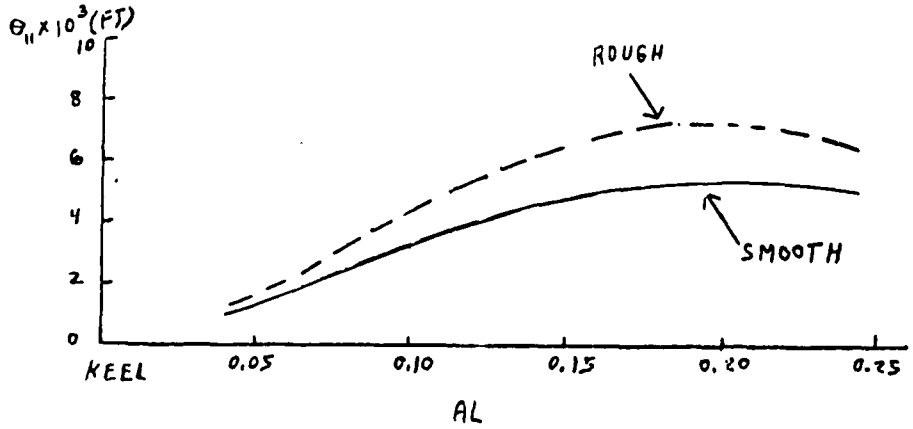

Figure 2-6. Girthwise distribution of streamwise momentum thickness θ_{11} for the elliptic cross-section ship model RL = 1 x 10^7.

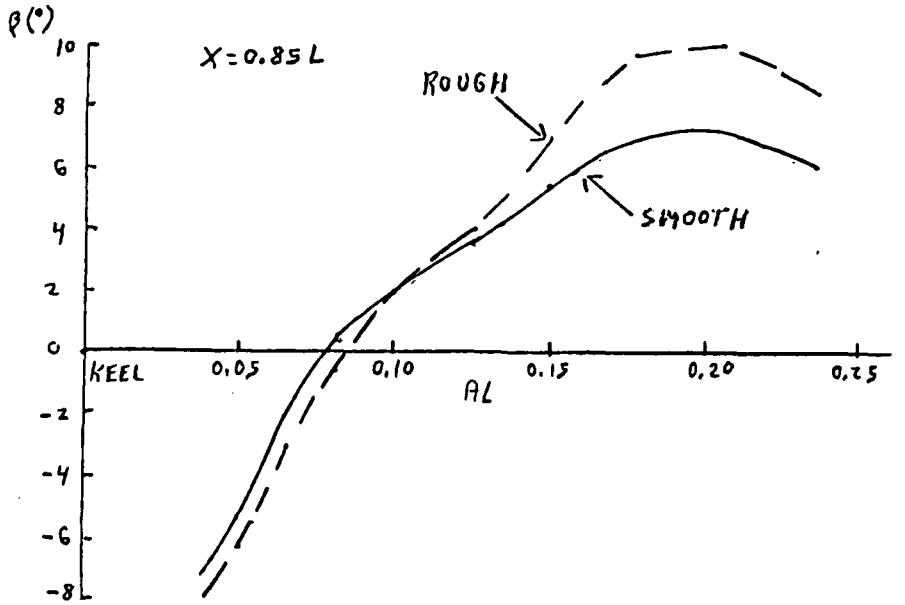

Figure 2-7. Girthwise distribution of cross-flow angle β for the elliptic cross-section model, RL = 1 x 10^7.

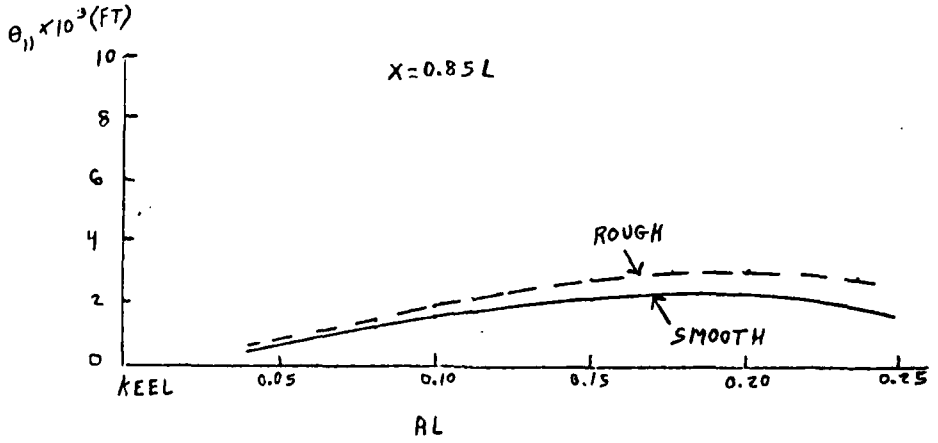

Figure 2-8. Girthwise distribution of momentum thickness θ_{11} for the elliptic cross-section ship, RL = 2 x 10^9.

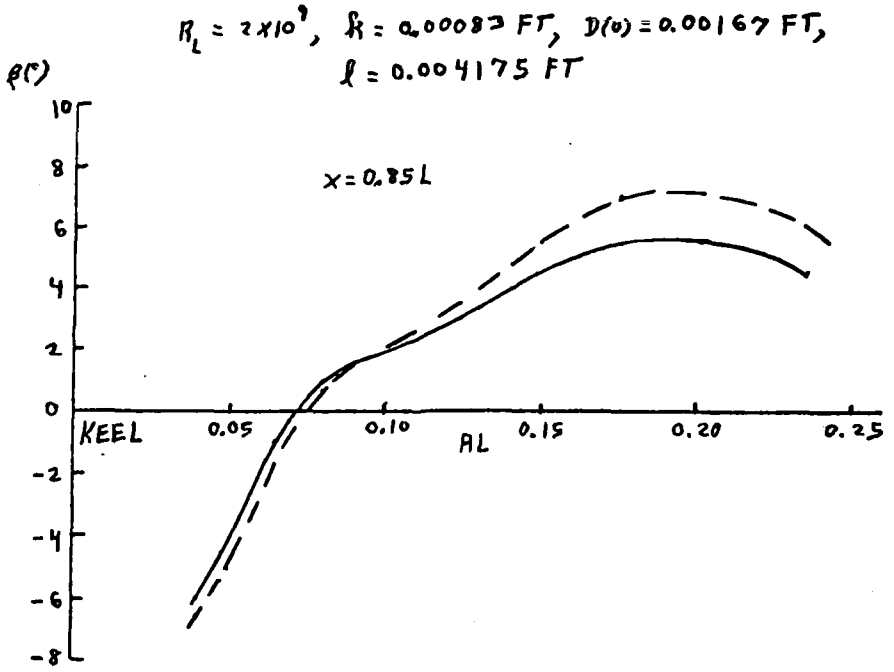

Figure 2-9. Girthwise distribution cross-flow angle β for the elliptic cross-section ship, RL = 2 x 10^9.

3.0 VISCOUS-INVISCID INTERACTIONS

3.1 Introduction

It has been well established now that the stern boundary layer and near wake cannot be handled by classical boundary layer theory alone (see Larson, 1981 and Patel, 1983). The stern boundary layer is fairly thick and causes a considerable disturbance to the bare body potential flow. There are two currently popular ways to deal with the stern flow. One way is by using boundary layer theory with viscous-inviscid interactions and the other way is by abandoning the boundary layer equations in favor of the "Parabolized Navier-Stokes" (PNS) equations (see, for example, Hogan, 1983). The latter method is very complex and relies more heavily on large computers and computing budgets. In keeping with the overall simplicity and practicality of the momentum integral method it is desirable to develop a relatively simple way to do viscous-inviscid interaction calculations. It is not expected that such a method will be as accurate as PNS calculations (if they ever do become fully developed) or even viscous-inviscid interaction methods based on finite differenced full higher order boundary layer equations (if these can ever be made to work for ship sterns), but at least a small improvement at the stern of the basically simple and practical momentum integral method seems worthwhile.

A considerable effort has been expanded to develop a momentum integral-based method of viscous-inviscid interaction. This effort was at first unsuccessful. (For completeness, a brief outline of this effort is given in the appendix.) Unfortunately, the limited budget of this contract did not allow completion of a new method which has been developed and is believed to hold considerable promise. This new method of viscous-inviscid interaction is detailed below. The method is based on the boundary layer momentum integral equations and slender body potential flow theory.

A word should be said here in defense of slender body potential flow theory. This theory has often been cited as being inadequate for describing the pressure distribution on bodies, particularly near the ends. This is only partially true. However, slender body theory need not be used to calculate the boundary layer over the first 60 to 80 percent of the body. There the boundary layer is thin and does not siginficantly interact with the body's potential flow. Hence, this part of the boundary layer can be calculated once and for all using an exact potential flow. The slender body theory only comes into play in the stern region. But there the viscous-inviscid interaction effectively smooths out the body, i.e., the displacement body is much smoother and more gently sloping than the actual body. Hence there is no reason to believe that slender body theory cannot accurately describe the potential flow over the displacement body. Furthermore, with slender body theory an infinite displacement body in the wake can be accounted for with no truncation.

The new viscous-inviscid interaction theory is described in the next two subsections. In order to clearly illustrate this theory, the axisymmetric case is treated first. Then extension to three-dimensional ship flows is outlined.

3.2 Axisymmetric Viscous-Inviscid Interactions

The starting point of this theory is the following physical picture of viscous-inviscid interaction employed successfully by Huang, et al. (1976). The boundary layer develops on the body defined by the radius $r_0(x)$, $x\varepsilon [x_n, x_t]$, where x is the axial coordinate, x_n is the body's nose location and x_t is the body's tail location. The boundary layer flow is driven downstream on the body by the inviscid flow corresponding to the displacement body defined by $r_0(x) + \delta_*(x) \cos\gamma$ where $\delta_*(x)$ is the effective displacement thickness and $\delta_*(x) \to \delta_\infty \neq 0$ for $x \to \infty$. Huang, et al. developed a method which relies on calculating the boundary layer only to the end of the body (or nearly to the end, say $x = b < x_t$). The extension of the displacement

thickness $\delta_*(x)$ into the wake is handled by an extrapolation polynomial which is controlled far downstream by an estimate of the total body drag. The iteration procedure to solve this problem is developed on the basis that successive calculated displacement bodies have the same pressure distribution. This method of iterating the boundary layer and potential flow seems to work fairly well even though it does not really converge very rapidly. The method seems to oscillate about a mean value of drag. Huang, et al., simply average these oscillations to obtain a fairly accurate final result. The method outlined below makes apparent why this type of method behaves in the way Huang, et al., discovered. It is noted here that almost all viscous-inviscid interaction methods seem to have such convergence problems. It is found that rather drastic under-relaxation needs to be used to make such methods converge (see, for example, Carter, 1978). This convergence problem may portend serious difficulties for 3-D flows. Such flows have an extra degree of freedom which usually results in more difficult convergence problems.

The starting point of this development is the slender body theory of Tuck and von Kerczek (1968). In polar coordinates with r denoting the radial and x the axial coordinates, the velocity potential is given explicitly by the formula

$$\phi = x + c(x)\ \ell n\ \tilde{r}_0(x) r - \tfrac{1}{2}\int_{x_n}^{\infty} dc(\xi)\ \mathrm{sgn}(x-\xi)\ \ell n\ 2|x-\xi| \qquad (3\text{-}1)$$

where $\tilde{r}_0(x) = r_0(x) + \delta_*(x)\cos\gamma$ ($\tilde{r}_0(x) = r_0(x)$ in the case of no viscous-inviscid interaction), $r = 1$ evaluates ϕ on the body $\tilde{r}_0$ and

$$c(x) = \tilde{r}_0(x)\,\frac{d\,\tilde{r}_0(x)}{dx}\,. \qquad (3\text{-}2)$$

The upper limit of the integral is x_t when $\delta_*(x) = 0$.

It should be noted that if the body has a blunt tail the potential (3-3) is very singular there, and hence the boundary layer on such bodies separates. This could prevent any viscous-inviscid interaction method from converging because a separated flow is not a suitable first guess. This can be overcome by artificially extending the body into the wake. This procedure can be carried out by the same method that is described below for extending the displacement surface into the wake. Thus, a way to obtain a suitable starting boundary layer needs no further discussion.

It is now assumed that calculations of the boundary layer have yielded the displacement surface

$$\tilde{r}_o(x) = r_o(x) + \delta_*(x) \cos\gamma \tag{3-3}$$

up to $x = b < x_t$ ($|(x_t - b)| \ll 1$) and where γ is the angle between the tangent to the body meridian and the x-axis. Then

$$c(x) = \tilde{r}_o \tilde{r}_o' = \frac{\Delta'}{2\pi} \tag{3-4}$$

where Δ is the cross-sectional area of the displacement body and primes denote differentiation with respect to x.

The slender body theory (3-1) requires that $c(x) \to 0$ as $x \to \infty$ in order that $\phi < \infty$. Thus it is best to work directly with extrapolating c(x) downstream rather than $\tilde{r}_o(x)$. From here on subscribts b denote evaluation at x = b.

The following inverse polynomial extrapolation has suitable behavior at $x \to \infty$ and can be matched to the displacement body at x = b:

$$2\pi\, c'(x) = \Delta''(x) = (\Delta_b'' + K)\left(\frac{b-\lambda}{x-\lambda}\right)^{2+\beta} - K\left(\frac{b-\lambda}{x-\lambda}\right)^{3+\beta} \tag{3-5}$$

where $\lambda < b$, $\beta > 0$ and K are adjustable parameters. Note that equation (3-5) satisfies the two requirements that $\Delta''(b) = \Delta''_b$ and $\Delta''(\infty) = 0$. By integrating

equation (3-5) twice and matching to the displacement body at $x = b$, the wake displacement body $\tilde{r}(x)$ is obtained. Thus,

$$2\pi c(x) = \Delta'(x) = -\frac{(\Delta''_b+K)(b-\lambda)}{(1+\beta)}\left(\frac{b-\lambda}{x-\lambda}\right)^{1+\beta} + \frac{K(b-\lambda)}{(2+\beta)}\left(\frac{b-\lambda}{x-\lambda}\right)^{2+\beta} \tag{3-6}$$

and

$$\Delta(x) = \Delta_b + \frac{(\Delta''_b+K)(b-\lambda)^2}{\beta(1+\beta)}\left[\left(\frac{b-\lambda}{x-\lambda}\right)^{\beta} - 1\right] - \frac{K(b-\lambda)^2}{(1+\beta)(2+\beta)}\left[\left(\frac{b-\lambda}{x-\lambda}\right)^{1+\beta} - 1\right] \tag{3-7}$$

where

$$K = -\frac{(2+\beta)}{(b-\lambda)}\left[(b-\lambda)\,\Delta''_b + (1+\beta)\,\Delta'_b\right]. \tag{3-8}$$

The evaluation of equation (3-7) for $x \to \infty$ yields the relationship between Δ_∞ and Δ_b, namely

$$\Delta_\infty = \Delta_b + \frac{2}{\beta}(b-\lambda)\,\Delta'_b + \frac{1}{(1+\beta)(2+\beta)}(b-\lambda)^2\,\Delta''_b. \tag{3-9}$$

This extrapolated wake is C^2 continuous (i.e., Δ, Δ', Δ'' are continuous) at $x = b$. Thus, since the quantities Δ_b, Δ'_b and Δ''_b are computed by boundary layer theory it is expected that wake (3-7) is an accurate approximation of the wake in a significant neighborhood of the point $x = b$. If equation (3-7) departs significantly from the asymptotic shape of the wake, the departure should not have too much of an effect on the potential flow velocities upstream of and at the point b.

It is known (see Schlichting, 1979) that the far wake displacement area Δ_∞ is related to the drag coefficient C_D of the body by the equation

$$\Delta_\infty = \frac{A_o}{4} C_D. \tag{3-10}$$

where A_o is the body reference area. Hence, equation (3-9) yields the relationship

$$A_o C_D = 4\Delta_b + \frac{8}{\beta}(b-\lambda)\,\Delta_b' + \frac{4}{(1+\beta)(2+\beta)}(b-\lambda)^2\,\Delta_b'' \qquad (3\text{-}11)$$

which will be the basis of the iteration procedure for calculating the viscous-inviscid interaction.

However, before describing this iteration procedure in detail it is best to carry equation (3-11) a little further. The axisymmetric momentum integral boundary layer equations are the following:

$$\frac{d\Theta}{ds} + \Theta(2+H)\frac{1}{U}\frac{dU}{ds} = \tfrac{1}{2}\, r_o(x)\, c_f \qquad (3\text{-}12a)$$

$$\frac{dQ}{ds} + Q\,\frac{1}{U}\frac{dU}{ds} = (\delta\cos\gamma + r_o)\, F(G) \qquad (3\text{-}12b)$$

where Θ is the momentum area, $H = \Delta_*/\Theta$, Δ_* is the displacement area (note $\Delta_* \neq \Delta$), $Q = \Theta G$, G is Head's shape parameter, s is arclength along a body meridian, c_f is the skin friction coefficient, F is the entrainment rate and U is the potential flow speed on the displacement body. See K for the details of these boundary layer equations. The arclength s and the axial coordinate x are related by

$$ds = \sqrt{1 + r'(x)^2}\; dx. \qquad (3\text{-}13)$$

In the vicinity of the tail of the body

$$r_o \approx 0$$

$$c_f \approx 0$$

$$ds \approx dx \;(\text{or } \gamma_b\, dx)$$

and

$$H \approx \text{constant} = H_b.$$

Thus, the momentum equation (3-12a) reduces there to the equation

$$\Delta' + \Delta(2+H_b)\, U'/U = 0. \tag{3-14}$$

By evaluating this equation at $x = b$, the following relationships are obtained:

$$\Delta_b' = -\frac{(2+H_b)\, U_b'}{U_b}\, \Delta_b \tag{3-15a}$$

and

$$\Delta_b'' = \frac{(2+H_b)}{U_b^2}\left[U_b''\, U_b + (3+H_b)\, U_b'^{\,2}\right]\Delta_b\ . \tag{3-15b}$$

Hence, equation (3-11) can be rewritten as

$$A_o\, C_D = 4\, \Delta_b \left\{1 - \frac{2}{\beta}\,(b-\lambda)\,\frac{(2+H_b)}{U_b}\, U_b' + \frac{(b-\lambda)^2(2+H_b)\left[(3+H_b)\, U_b'^{\,2} - U_b''\, U_b\right]}{(1+\beta)(2+\beta)\, U_b^2}\right\}. \tag{3-16}$$

Equation (3-16) clearly brings out the direct and seemingly sensitive dependence of C_D on U_b, U_b' and U_b''. In fact, it seems likely that a good choice of λ is such that $(b-\lambda) = \frac{1}{2}$, say, and that probably $\beta = O(1)$. Then the third term in equation (3-16) is probably negligible. It is then fairly easy to see that viscous-inviscid iteration schemes will oscillate at each iteration. Equation (3-16) is approximately the same as

$$A_o\, C_D = 4\, \Delta_b\left(1 - \frac{(2+H_b)}{\beta U_b}\, U_b'\right), \tag{3-17}$$

and under the same assumptions, equation (3-11) is approximated by

$$A_o\, C_D = 4\, \Delta_b + \frac{8}{\beta}\, \Delta_b'\ . \tag{3-18}$$

Assume that n is the iteration number. If at iteration n the value of $\Delta'_{bn} > 0$, then it will produce a new velocity $U'_{bn+1} > 0$. Then if this new velocity distribution for which $U'_{bn+1} > 0$ is used to recalculate the boundary layer, producing Δ'_{bn+1}, then by equations (3-17) and (3-18) (and also simple physical reasoning) it is evident that $\Delta'_{bn+1} < 0$. Thus, it is apparent that viscous-inviscid iteration will always lead to oscillatory convergence (or divergence).

It is now worthwhile to state the iteration algorithm for viscous-inviscid interaction calculations.

Step 0: $\tilde{r}_o(x) = \begin{cases} r_o(x) & x_n \leq x \leq x_t \\ o & x > x_t \end{cases}$

If body is very blunt at the tail, possibly causing boundary layer separation, add an artificial tail to the body using wake formulas (3-5) - (3-7) with $b = x_t - \varepsilon$, $\varepsilon > 0$, $r_{ob} = \tilde{r}_o(x_t - \varepsilon)$ and $c'_b = c'(x_t - \varepsilon)$ and replacing $\tilde{r}_o(x) = 0$ with $\tilde{r}_o(x) =$ this artificial tail for $x > x_t$.

Calculate potential flow on this body (either exact or by slender body theory or a combination of these).

Step 1: Calculate boundary layer on body $r_o(x)$ to $x = b$ to get $\Delta(x)$ and Δ_b, Δ'_b, Δ''_b.

Step 2: Construct wake function using Δ_b, Δ'_b, Δ''_b and calculate C_D from formula (3-11). Is $C_D = C_D$ from previsou iteration? (if on first step go to 3) Yes; go to step 4. No; go to step 3.

Step 3: Calculate U by slender body theory potential (3-1) using $\Delta(x)$ on body/wake from steps 1 - 2. Go to step 1.

Step 4: Calculate C_D by stress integration. If C_D is same as wake C_D problem is finished. If not, adjust λ(or β) so that the two values of C_D are equal and restart at step 2.

3.3 Three-Dimensional Viscous-Inviscid Interactions

The beauty of the theory outlined in the previous subsection is that it can be applied with only minor modifications to a ship hull. The starting point of this development is the representation of a ship hull by conformal mapping functions (von Kerczek and Tuck, 1969) and the general ship slender body theory (Tuck and von Kerczek, 1968).

The ship hull is given by r=1 in the equation

$$\vec{r}_o(x,\theta,r) = x\vec{i} + y(x,\theta,r)\vec{j} + z(x,\theta,r)\vec{k}. \tag{3-19}$$

In equation (3-19)

$$y + iz = \sum_{n=1}^{N} a_n(x)\zeta^{(3-2n)} \tag{3-20}$$

where

$$\zeta = re^{i\theta}$$

and $a_n(x)$ are interpolation functions along the axis of the ship.

The slender body velocity potential $\phi(x,r,\theta)$ is obtained directly in terms of the coefficient functions $a_n(x)$ by the following formulas: (Tuck and von Kerczek, 1968)

$$\phi = x + c_o(x)\ \ell n\ a_1(x)\zeta - \sum_{n=1}^{N-1} \frac{c_n(x)}{2n}\ \zeta^{-2n} - \tfrac{1}{2}\int_{x_n}^{\infty} d\ c_o(\xi)\ \mathrm{sgn}(x-\xi)\ \ell n 2|x-\xi| \tag{3-21}$$

where the coefficients $c_n(x)$, n = 0, ..., N are obtained from the formulas

$$c_n = (\gamma_n + \gamma_{-n})\ e_n \tag{3-22a}$$

$$\gamma_n = \sum_{\ell=1}^{N-n} (3-2\ell)\ a_\ell(x)\ a'_{\ell+n}(x) \tag{3-22b}$$

$$e_n = \begin{cases} \frac{1}{2} & \text{for } n = 0 \\ 1 & \text{for } n > 0 \end{cases} \qquad (3\text{-}22c)$$

and $$a_n(x) \equiv 0 \quad \text{for } n < 1 \text{ and } n > N.$$

The potential (3-22) splits into two important and distinct parts. The first three terms of equation (3-22) are local. They only depend on the particular point on the hull at which the velocity is evaluated. It is only this local group of terms that contains the entire non-axisymmetry of the hull shape. The integral in equation (3-22) is the only term that conveys the global aspects of the hull to each point on the ship. This term is exactly the same as in the axisymmetric case. The function $c_0(x)$ is the x-derivative of the cross-section area divided by 2π. Thus, the effects of the wake are felt on the hull only by its section area distribution, not its cross-section shape. This feature of slender body theory is the crucial element that makes the axisymmetric interaction theory easily extendable to three dimensions.

After the boundary layer is calculated, a displacement thickness distribution $\delta_*(x,\theta)$ is obtained. Since this displacement thickness is supposed to represent a distance normal to the hull, the equivalent distance normal to the cross section out to the effective displacement surface is given by $\delta_{*_c}(x,\theta)$ where

$$\delta_{*_c}(x,\theta) = \delta_*(x,\theta)(\vec{n}_c \cdot \vec{n}), \qquad (3\text{-}23)$$

where $\vec{n}$ is the unit normal vector to the hull and $\vec{n}_c$ is the unit normal vector to the cross-section. Furthermore, near the stern the value of δ_{*_c} may be so large that if this distance is plotted normal to the cross-section, the neighboring displacement distances would cross, as sketched in the figure below.

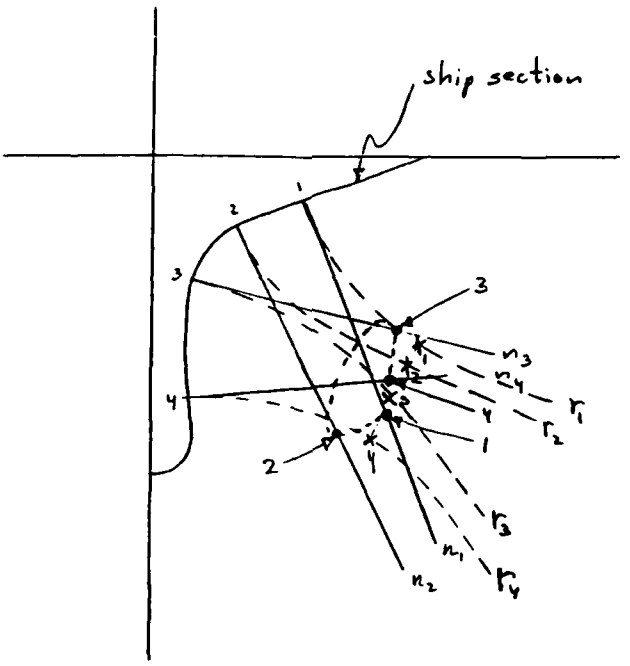

Schematic diagram showing inversion of outer edge of boundary layer when plotted as a function of distance along the normals (points denoted by dots, •) as opposed to the distance along the coordinates r (points denoted by x's).

This difficulty is easily overcome by plotting the displacement thickness along the r-coordinate curves (θ = constant) in the cross-sections. The cross-section equation (3-21) is a conformal mapping, hence the θ = constant curves are locally orthogonal to the cross-sections (r = constant = 1). Thus, if h_r denotes the metric coefficient of the r-coordinate, then at each station x the displacement surface $\vec{r}_d(x,\theta)$ is obtained by

$$\vec{r}_d(x,\theta) = \vec{r}_o(x,\theta,r_\delta) \tag{3-24}$$

where

$$\delta_{*c}(x,\theta) = \int_1^{r_\delta(x,\theta)} h_r(x,\theta)\, dr. \tag{3-25}$$

For the case where δ_{*c} is small enough not to cause the problems exhibited in the figure, the displacement surface can be obtained simply as

$$\vec{r}_d(x,\theta) = \vec{r}_o(x,\theta,1) + \delta_{*c}(x,\theta)\, \vec{n}_c. \tag{3-26}$$

Once the surface $\vec{r}_d(x,\theta)$ for $x\varepsilon[a,b]$ has been constructed, then the cross-sections of this surface are mapped onto the unit circle (using the von Kerczek-Tuck, 1969, algorithm) and a new set of mapping coefficients $a_n(x)$ is obtained. From these coefficients the new set of coefficients $c_n(x)$ are computed by formulas (3-22).

Now the section area derivative $c_0(x)$ must be extrapolated to infinity to complete the data for the potential (3-21). Again formulas (3-5) - (3-11) are used for the wake. The same algorithm that was used for the axisymmetric wake can now be used. Of course, the fully 3-D boundary layer calculation method of K (or any other 3-D boundary layer method) must be used to obtain the new effective displacement thickness $\delta_*(x,\theta)$.

The beauty of this method is that the actual cross-section shape of the wake need not be known as long as the potential flow velcoity on the wake displacement surface does not have to be computed. This is precisely what is achieved by extrapolating the wake cross-section area. Slender body theory makes this possible. It should be emphasized that this theory does not assume that the wake is axisymmetric. Use of slender body theory for the potential flow simply obviates the necessity to know the cross-section shape of the wake. This method for doing three-dimensional viscous-inviscid interaction seems extremely promising. Implementation of the method to bring it to fruition is planned.

4.0 COMPUTATIONAL IMPROVEMENTS TO THE BASIC MOMENTUM INTEGRAL METHOD

It was found, in the course of several applications of the method K, that the integration of the boundary layer equations broke down prematurely near the stern. This breakdown was traced to two causes. The first cause was an inadequate handling of the equations on the symmetry plane. The second cause was the requirement in the original program that the boundary layer equations be integrated with an axial step size conforming to the potential flow panels. The remedies to these difficiencies which required considerable effort are described below.

The original computer program of K (see von Kerczek, 1983) implemented the symmetry plane conditions by appropriate parity of the finite difference formulas on these planes (the load waterline and keel). It was found that this kind of implementation of symmetry plane conditions allows the boundary layer solution off the symmetry plane to affect the symmetry plane solution. But boundary layer theory indicates that the flow along a symmetry plane is completely independent of the flow elsewhere on the body (unless viscous-inviscid interactions are present). Hence, the symmetry plane boundary layer equations must be solved independently of the rest of the boundary layer and the results must be used as lateral boundary conditions to the full three-dimensional equations. This method of handling the symmetry planes has now been implemented in the method of K and results in improved predictions of the boundary layer.

The original computer program for the method of K used axial step sizes fixed to the potential flow panels. The potential flow panels cannot be made small enough at a ship stern to accommodate the requirements of the boundary layer equations unless an enormously expensive potential flow calculation can be tolerated. This problem was alleviated by writing a preprocessor that interpolates the potential flow data onto an arbitrary grid. This decouples the numerical algorithm for solving the boundary layer equations from the potential flow panels. The boundary layer equations in K can

now be integrated on very fine step sizes near the stern of a ship. This greatly improves the performance of the code of K. For example, the boundary layer can now be computed to within 2% of ships' length to the stern of the semi-elliptic hull of Huang, et al. (1976). Comparison of such calculations with the experimental data of Huang, et al. is not shown here because the experiments had insufficient detail to allow the discernment of an appropriate set of initial conditions to start the calculations. The calculations that were made used rough guesses for initial conditions, and thus the results, though qualitatively correct, are not comparable to the experimental data.

It is planned that the SSPA model boundary layer (see K) will be recalculated and compared to experiment with the improved code described above.

APPENDIX: UNSUCCESSFUL METHOD FOR CALCULATING VISCOUS-INVISCID INTERACTING AT A STERN

A brief outline is given here describing an unsuccessful idea for calculating the stern flow of ships. This outline is given mainly to illustrate the difficulties that are inherent in trying to join computationally the boundary layer and near wake calculations. The difficulties lie mainly in trying to match up two geometrically dissimilar regions. It was shown in Section 3 that a viscous-inviscid interaction scheme will be very sensitive to the potential flow velocity and its first two derivatives. This forebodes difficulties for any method that attempts to actually match up surfaces in three dimensions.

The idea in the first attempt to do viscous-inviscid interactions was to model the displacement effects by a distribution of extra sources on the body and its extension in the wake. This attempt was carried out on the Groves, et al. (1982) semi-elliptic body.

The body was truncated at a station $x_t - \varepsilon$, $0 < \varepsilon << 1$, and an elliptic cross-section tail cone was attached there. This tail cone extended a distance downstream determined at $x = x_t - \varepsilon$ by the slopes of the waterline and keel of the actual body.

The first iteration calculated the full three-dimensional bare body boundary layer up to station $x_t - \varepsilon$. At station $x_t - \varepsilon$ onwards the wake was computed on the waterline and keel of the extended tail cone. The centerline pressure distribution behind the body without the tail cone was used for the wake calculation. The tail cone only serves the purpose of providing a continuation of the coordinate system off the end of the body.

This boundary layer and wake calculation then provides the displacement surface $\delta_*(x,\theta)$ (using the coordinates of section 3.2 say). Extra

sources,

$$\sigma = U \frac{\partial \delta_*}{\partial s} \tag{A-1}$$

where s is the arclength along the streamlines, were then distributed on the body and its extension. The increment to the original exact bare body potential flow was then computed by slender body theory. Using this new potential flow, the boundary layer and wake were recalculated.

The method failed because of extremely erratic behavior of the potential flow and the extra source strengths σ in the neighborhood of the tail of the body. Examination of the details of this method did not lead to optimism towards a continuation of this technique, so it was abandoned.

The lesson learned here is that it is very tricky to actually continue a three-dimensional body, even a displacement body, into the wake. The reason is that the potential flow is so sensitive to inflection points (i.e., in naval architectural terms, the fairness of the body) that it is too difficult to extend surfaces in three dimensions. The slender body method outlined in section 3.2 only requires that a curve be continued downstream, namely the section area curve. This is the same as what is required in the axisymmetric case, and this has been shown to work by Huang, et al. (1976).

REFERENCES

Betterman, D. (1966) "Contribution a l'Etude de la Connection Forces Turbulente le long Plaques Rugueuses," Int. J. Heat & Mass Transfer, Vol. 9, pp. 153-164.

Carter, J.E. (1978) "A New Boundary Layer Interaction Technique for Separated Flows," NASA-TM-78690.

Christoph, G.H., and R.H. Pletcher (1983) "Prediction of Rough-Wall Skin Friction and Heat Transfer," AIAA Journal, Vol. 21, No. 4, pp. 509-515.

Dirling, R.B., Jr. (1973) "A Method for Computing Roughwall Heat Transfer Rates on Re-entry Nosetips," AIAA Paper No. 73-763, presented at the AIAA 8th Thermophysics Conference, Palm Springs, CA, 16-18 Jul 1973.

Finson, M.L. (1982) "A Model for Rough Wall Turbulent Heating and Skin Friction," AIAA Paper No. 82-0199, presented at AIAA 20th Aerospace Sciences Meeting, Orlando, FL, 11-14 Jan 1982.

Finson, M.L., and A.S. Clarke (1980) "The Effect of Surface Roughness Character on Turbulent Re-entry Heating," AIAA Paper No. 80-1459.

Granville, P.S. (1974) "A Modified Froude Method for Determining Full Scale Resistance of Surface Ships from Towed Models," J. Ship Res., Vol. 18, No. 4.

Groves, N.C., G.S. Belt and T.T. Huang (1982) "Stern Boundary Layer Flow on a Three-Dimensional Body of 3:1 Elliptic Cross Section," Report #DTNSRDC-82/022.

Healzer, J.M., R.J. Moffat and W.M. Kays (1974) "The Turbulent Boundary Layer on a Porous Rough Plate: Experimental Heat Transfer with Uniform Blowing," AIAA Paper No. 74-680 and ASME Paper No. 74-HT-14, presented at the AIAA/ASME 1974 Thermophysics and Heat Transfer Conference, Boston, MA, 15-17 Jul 1974.

Hogan, T.F. (1983) "A Calculation of the Parabolized Navier-Stokes Equations for Turbulent Axisymmetric Flows Using Streamline Coordinates and the k-ε Turbulence Model," DTNSRDC Report #83/070.

Huang, T.T., et al. (1976) "Propeller/Stern/Boundary-Layer Interaction on Axisymmetric Bodies: Theory and Experiment," DTNSRDC Report #76/0113.

Larsson, L. (ed.) (1981) "SSPA-ITTC Workshop on Ship Boundary Layers 1980," SSPA, Goteborg, Report No. 90.

Lin, T.C., and R.J. Bywater (1982) "Turbulence Models for High-speed, Rough-wall Boundary Layers," AIAA Journal, Vol. 20, No. 3, pp. 325-333.

Patel, V.C. (1983) "Some Aspects of Thick Three-Dimensional Boundary Layers," Proc. 14th Symp. Naval Hydrodynamics, National Academy Press, Washington, D.C.

Schlichting, H. (1937) "Experimental Investigation of the Problem of Surface Roughness," NACA TM823.

Schlichting, H. (1969) Boundary Layer Theory, McGraw-Hill, New York.

Simpson, R.L. (1973) "A Generalized Correlation of Roughness Density Effects on the Turbulent Boundary Layer," AIAA Journal, Vol. 11, No. 2, pp. 224-244.

Stern, F., and C. von Kerczek (1983) "Calculation of Appendage Drag and Propeller Inflow for Destroyer Hull Forms," NAVSEA Tech. Note 051-55W-TN0002.

Tuck, E.O., and C. von Kerczek (1968) "Streamlines and Pressure Distribution on Arbitrary Ship Hulls at Zero Froude Number," J. Ship Res., Vol. 12, No. 3.

von Kerczek, C.H. (1982) "A New Generalized Cross-Flow Momentum Integral Method for Three-Dimensional Ship Boundary Layers," SAI Report #463-82-085-LJ.

von Kerczek, C.H. (1983) "A User's Manual for the Ship Boundary Layer Program GHRBLD," Supplement to SAI Report #463-82-085-LJ for Contract #N00014-81-C-0234.

von Kerczek, C., and T. Langan (1979) "An Integral Prediction Method for Three-Dimensional Turbulent Boundary Layers on Ships," DTNSRDC Report #79/006.

von Kerczek, C., C. Scragg and F. Stern (1983) "A Comparative Study of the Resistance of Two Destroyer Hull Forms," NAVSEA Technical Note #051-55W-TN0001.

von Kerczek, C., and E.O. Tuck (1969) "The Representation of Ship Hulls by Conformal Mapping Functions," J. Ship Res., Vol. 13, No. 4.

END

FILMED

4-85

DTIC